ELSEVIER

Biochimica et Biophysica Acta 1369 (1998) 131–140

BIOCHIMICA ET BIOPHYSICA ACTA
BBA

Helicity, membrane incorporation, orientation and thermal stability of the large conductance mechanosensitive ion channel from *E. coli*

Isaiah T. Arkin [a,1], Sergei I. Sukharev [b,2], Paul Blount [b], Ching Kung [c], Axel T. Brünger [a,*]

[a] *Department of Molecular Biophysics and Biochemistry, Howard Hughes Medical Institute, Yale University, New Haven, CT 06520, USA*

[b] *Laboratory of Molecular Biology University of Wisconsin-Madison, Madison, WI 53706, USA*

[c] *Department of Genetics, Laboratory of Molecular Biology, University of Wisconsin-Madison, Madison, WI 53706, USA*

Received 18 June 1997; revised 11 August 1997; accepted 19 August 1997

Abstract

In this report, we present structural studies on the large conductance mechanosensitive ion channel (MscL) from *E. coli* in detergent micelles and lipid vesicles. Both transmission Fourier transform infrared spectroscopy and circular dichroism (CD) spectra indicate that the protein is highly helical in detergents as well as liposomes. The secondary structure of the proteins was shown to be highly resistant towards denaturation (25–95°C) based on an ellipticity thermal profile. Amide H^+/D^+ exchange was shown to be extensive (ca. 66%), implying that two thirds of the protein are water accessible. MscL, reconstituted in oriented lipid bilayers, was shown to possess a net bilayer orientation using dichroic ratios measured by attenuated total-reflection Fourier transform infrared spectroscopy. Here, we present and discuss this initial set of structural data on this new family of ion-channel proteins. © 1998 Elsevier Science B.V.

Keywords: Ion channel; Membrane protein; Fourier transform infrared spectroscopy (FT-IR); Circular dichroism; Lipid bilayer

1. Introduction

The extracellular environment constantly challenges microorganisms, as they have little control over it. Osmotic stress, resulting from hypertonic or hypotonic pressure, can irreversibly harm a microorganism if it does not possess the capability to respond to it immediately. One such response may be in the form of an ion channel gated by osmotic pressure. Thus, osmotic pressure would open a *mechanosensitive* channel, thereby allowing ions and small osmolytes to traverse the channel according to their electrochemical gradient, and concomitantly collapsing the osmotic stress.

Recently, single-channel recordings were able to identify two distinct levels of current that are generated by a pressure gradient across the patch membrane [1]. The proteins responsible for these currents were, therefore, mechanistically termed MscL and MscS: mechanosensitive channel of large conductance and mechanosensitive channel of smaller conductance, respectively. Attempts to purify and se-

Abbreviations: CD, circular dichroism spectroscopy; DMPC, dimyristoylphosphocholine; MscL, large conductance mechanosensitive ion channel

* Corresponding author. Fax: +1 203 432 6946.

[1] Present address: Cambridge University, Department of Biochemistry, 80 Tennis Court Road, Cambridge CB2 1GA, UK.

[2] Present address: University of Maryland, Department of Zoology, College Park, MD 20742, USA.

PII S0005-2736(97)00219-8

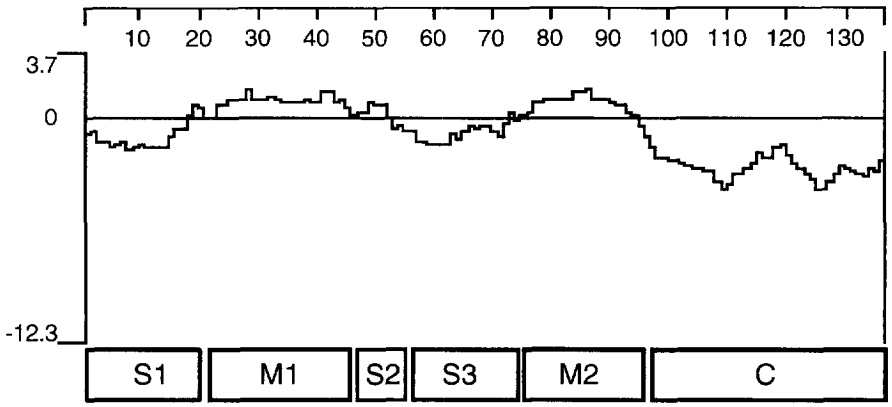

Fig. 1. A schematic diagram indicating the different segments of MscL, obtained by a hydrophobicity analysis using the Goldman–Engelman–Steitz [29] scale with a window of 20 amino acids. The letters 'S' designate surface elements, 'M' membranous elements and 'C' the carboxy terminal part of the protein.

quence the MscL channel were successful and have led to the determination of the first sequence from this new family of ion-channel proteins [2].

The protein was shown to have a sequence dissimilar to any other ion-channel family, and was divided into five elements based on hydrophobicity analysis (shown schematically in Fig. 1). Elements M1 and M2 are highly hydrophobic and were, therefore, predicted to be membrane embedded, while elements S1, S2, S3 and C are hydrophilic and are presumed to be extramembranous. The presence of a few charged residues and the length of the hydrophobic segments precludes automatic assignment of these membranous domains as putative transmembrane α-helices or of a β-strand forming a β-barrel. This finding is distinct from most other ion channels, where putative transmembrane helical bundles are readily visible just from sequence inspection.

Recently, Blount et al. [3] localized MscL to the inner membrane of *E. coli* and, by PhoA fusion, have shown that it contains two transmembrane domains with both, amino and carboxy termini on the cytoplasmic side. Cross-linking results have indicated that the active complex is a homo-hexamer. The lack of sequence similarity to other known channels, the gating by tension in the lipid bilayer, and the extremely high unitary conductance (ca. 3 nS in 300 mM KCl) with no selectivity [1], implying a wide pore, all suggest that the MscL channel may represent a novel structural design.

Here, to gain direct structural insights into this new family of ion-channel proteins, we have obtained Fourier transform infrared, attenuated total-reflection Fourier transform infrared and CD spectra of affinity purified MscL. MscL was found to be a highly helical protein with predominant trans-bilayer orientation, consistent with the previous helix–loop–helix structural model [3]. About two thirds of all amide protons were readily exchangeable for deuterium, indicative of their surface accessibility. A high stability of MscL secondary structure to denaturing factors was observed, a finding that is typical for highly hydrophobic membrane-embedded proteins. We discuss possible structural implications of these unusual properties of the MscL protein.

2. Materials and methods

2.1. Protein purification and reconstitution

2.1.1. MscL histidine tagging

A tag of six sequential histidines was added to the C-terminal end of the MscL open-reading frame (ORF) by a two-step amplification using PCR [4]. Starting with the MscL ORF (insert of the 5-2-2 plasmid [2]) as template, the MscL ORF was amplified using the 5′ primer used previously to amplify the 5-2-2, and with the following oligonucleotide as the 3′ primer: GAT GAT GAT GAT GAT GAG AGC GGT TAT TCT GCT C. The resulting product was gel purified using Geneclean II (BIO101, Vista,

CA) and used as template for a subsequent amplification using the same 5′ primer, and another 3′ primer with the sequence CTC GAG TTA ATG ATG ATG ATG ATG ATG AGA. This latter product was subcloned, using XhoI, into the pB10a expression vector [2]; the final product was called MscL-6His.

2.1.2. Protein purification

For protein purification, the PB101 strain (mscL-[2]) carrying the MscL-6His construct was grown in LB (40 l fermentor) and induced for 4 h with 0.8 mM IPTG. Cells were French-pressed and membranes were isolated by differential centrifugation, as previously described [2]. The membrane pellet (5–8 g wet weight) was solubilized in 100 ml of extraction buffer (50 mM $Na_2HPO_4 \cdot NaH_2PO_4$, 300 mM NaCl, 35 mM imidazole) containing 3% *n*-octyl β-glucoside, and 1 mM phenylmethylsulfonyl fluoride. The extract was cleared by centrifugation at $120000 \times g$ for 35 min, mixed with 8 ml (bed volume) Ni^{2+}-NTA agarose beads (Qiagen, Chatworth, CA) equilibrated in the same buffer and gently rotated for 15 min (batch-loading). The column was then packed in a 15 ml shell with an upper flow adapter, extensively washed with the wash buffer, (same as extraction buffer, with 1% *n*-octyl β-glucoside) and the bound proteins were then eluted with a 30 min linear gradient of imidazole (35 to 500 mM, 1 ml/min) followed by a sustained wash with 500 mM imidazole for another 10 min. When stated, detergent exchange from *n*-octyl β-glucoside to *n*-dodecyl-β-D-maltoside was achieved by washing the column with 8–10 bed volumes of the wash buffer containing 0.1% *n*-dodecyl-β-D-maltoside followed by the imidazole gradient elution in the presence of the same detergent.

The 6His-tagged MscL was eluted in the last third of the gradient, yielding ≈ 2 mg of pure protein as estimated by the modified Bradford method [5] and the micro-BCA assay (Pierce, Rockford, IL) recalibrated in the presence of each detergent. The MscL-6His content in individual fractions was examined using 12% sodium dodecyl sulfate–polyacrylamide minigels and estimated to be > 98% pure in the final pool of fractions. To avoid high concentration of imidazole in optical samples, the protein was concentrated on a Centriplus 30 concentrator (Amicon, Beverly, MA) and finally transferred into 20 mM phosphate buffer with either 1% *n*-octyl β-glucoside or 0.1% *n*-dodecyl-β-D-maltoside by 'gel-filtration' on a PD10 column (Pharmacia, Uppsala, Sweden). At this point the presence of endogenous lipid is negligible.

2.1.3. Protein reconstitution

An aliquot, 250 μl of a solution containing 25 mg/ml DMPC (Avanti Polar Lipids, Alabaster, AL) and 5% *n*-octyl β-glucoside, was added to the solution of the protein (500 μl at 10–50 μM) in *n*-octyl β-glucoside (Sigma, St. Louis, MO). Subsequent reconstitution of the peptides into phospholipid vesicles was achieved by exhaustive dialysis into a buffer containing 0.1 mM $Na_2HPO_4 \cdot NaH_2PO_4$ pH 6.8 and 125 μM EDTA · HCl. Final protein-to-lipid molar ratio was roughly 1 : 100. The DMPC/MscL vesicles were used for the Fourier transform infrared spectroscopy (FT-IR) studies described below.

2.2. CD spectroscopy

CD measurements were performed on an Aviv 62DS and 60DS circular dichroism spectrometers (Lakewood, NJ) using a 1 mm path length cuvette (Helma, Jamaica, NY). Spectral averaging was used to increase signal-to-noise ratio, as indicated in the figure legends. The samples were diluted as mentioned into water and protein concentrations (0.8–8 μM) were determined by internally standardized amino acid analysis following acid hydrolysis (carried out by the W.M. Keck Foundation Biotechnology Resource Laboratory at Yale University), modified Bradford method [5] and the Pierce BCA assay, all yielding similar results to within 15%. The CD spectra obtained for MscL in sodium dodecyl sulfate was obtained for the identical sample in 1% *n*-β-octyl glucoside micelles followed by addition of sodium dodecyl sulfate to a final concentration of 2%. The sample was then boiled for 40 min and allowed to cool to room temperature overnight in order to ensure complete solvation by the detergent. Samples in 0.1% *n*-dodecyl-β-D-maltoside were obtained by detergent exchange on the metal chelating resin as stated above. The CD spectra shown are an averaged result of more than three different experiments each yielding nearly identical results.

For the CD thermal profile, the wavelength was held at 222 nm and the protein concentration was

≈ 2.0 μM. The temperature step was 1°C, followed by 1 min of equilibration and 5 s of averaging at each temperature point. Sample evaporation was prevented by a Teflon stopper and Parafilm coating.

2.3. Transmission Fourier transform infrared spectroscopy

A Nicolet Magna 550 spectrometer (Madison, WI) purged with N_2 and equipped with a mercury–cadmium tellurium detector was used for recording Fourier transform infrared spectra. For each sample, 1000 interferograms recorded at a spectral resolution of 4 m^{-1} were averaged. Interferograms were processed using 1-point zero filling and Happ–Genzel apodization, followed by automatic base line correction (provided in the OMNIC software by Nicolet, Madison, WI). Fourier self-deconvolution, a process involving a deconvolution of the spectra from its 'inherent' line shape [6], was performed using the OMNIC software package from Nicolet (Madison, WI) with a bandwidth of 13 cm^{-1}. An enhancement factor of 2.4 was used in the deconvolution, determined previously to best fit experimental data [7].

Spectra were obtained by drying 50 μl of sample (protein concentration of 10–50 μM) on Ge windows (13 × 2 mm, Grasbey Specac, Kent, UK) with dry air. Exchange of the solvent from H_2O to D_2O was achieved by centrifuging the sample (400 μl, 10–50 μM) for 1 h in an A-95 rotor at 178 000 × g using an Airfuge ultracentrifuge (Beckman, Palo Alto, CA). Pellets were resuspended in 75 μl of either H_2O or D_2O. The sample was then dried down after 2 h of incubation. The phase of the lipid at the time of the experiment was that of gel phase.

Analysis of secondary structure content was based on the methodology developed by Venyaminov and Kalnin [8–10] and recently applied to several membrane proteins [11–13]. Briefly, this method takes into account the different extinction coefficients of the secondary structure elements as well as overlapping side-chain modes. In this method, the Fourier self-deconvoluted spectra in the amide I region (1600–1700 cm^{-1}) is divided into three segments, 1600–1647, 1647–1665 and 1665–1700 cm^{-1}. The only vibrational modes that would contribute to the absorption in the middle region (1647–1665 cm^{-1}) would be α-helical amide I modes, while the other two regions contain contributions from amide I modes of other secondary structure modes as well as side-chain modes. Since the number of each side-chain mode is known from the sequence, it is possible to estimate the α-helix, β-sheet and random coil content by solving a system of four coupled equations, yielding the protein concentration as well as the fractional content of each of the secondary structures present in the protein.

2.4. Attenuated total-reflection Fourier transform infrared spectroscopy

In order to collect attenuated total-reflection FT-IR spectra, the spectrometer was equipped with a wire grid polarizer (0.25 μm spacing, Grasbey Specac, Kent, UK). The sample (400 μl, 10–50 μM) was dried on the surface of a Ge internal-reflection element (52 × 20 × 2 mm) and, subsequently, hydrated with 100 μl of D_2O. Finally, the sample was placed in a 25 reflections variable-angle attenuated total-reflection accessory (Grasbey Specac, Kent, UK), and background subtraction was performed against D_2O.

2.4.1. Orientation analysis

The electric field components of the evanescent wave, $\mathscr{E}_x = 1.398$, $\mathscr{E}_y = 1.516$ and $\mathscr{E}_z = 1.625$ are given by Harrick [14]. These electric field components, together with the dichroic ratio (defined as the ratio between absorption of parallel ($A_{\parallel}$) and perpendicular ($A_{\perp}$) polarized light, $r^{atr} \equiv A_{\parallel}/A_{\perp}$), are used to calculate an order parameter defined as $\mathscr{S} = ([3 < \cos^2 \beta > -1]/2)$ with the following equation:

$$\mathscr{S} = \frac{\mathscr{E}_x^2 - R^{ATR}\mathscr{E}_y^2 + \mathscr{E}_z^2}{\mathscr{E}_x^2 - R^{ATR}\mathscr{E}_y^2 - 2\mathscr{E}_z^2}\left(\frac{3\cos^2\alpha - 1}{2}\right)^{-1}$$

where β is the angle between the helix director and the normal of the internal reflection element, and α the angle between the helix director and the transition dipole moment of the amide I vibrational mode, 39°C [15]. These equations are based on the reasonable assumption that the thickness of the deposited film (> 20 μm) is much larger than the penetration depth (ca. 1 μm) of the evanescent wave [14]. Using the values for the amplitudes of the evanescent wave given above as well as α, the equation reduces to $\mathscr{S}_{protein} = [2.4635R^{ATR} - 4.9252]/[R^{ATR} + 1.4631]$.

Order parameters of 1.0 and −0.5 correspond to helical orientations parallel, and perpendicular to the membrane normal, respectively. Lipid order parameters are obtained from the lipid methylene symmetric (2852 cm^{-1}) and asymmetric (2924 cm^{-1}) stretching modes using the same equation by setting $\alpha = 90°$, yielding the relationship between the order parameter and the dichroic ratio of $\mathscr{S}_{lipid} = [3.9986 - 2R^{ATR}]/[R^{ATR} + 1.4475]$.

3. Results and discussion

3.1. Secondary structure

3.1.1. CD

CD spectra in the far-UV regions (180–240 nm) have long been used as a convenient tool for estimating the secondary structure content of a protein. Quantitative analysis is performed by spectral deconvolution using basis sets of spectra obtained for 'pure' secondary structure elements. For example, the CD spectrum of an α-helix exhibits characteristic minima at 208 and 222 nm with magnitudes of $-36\,000 \pm 3000$ deg cm^2 $dmol^{-1}$, and a maximum at 190–195 nm with a magnitude of $70\,000 \pm 10\,000$ deg cm^2 $dmol^{-1}$ [16,17]. It is important to note that, in many cases in the literature, molar ellipticities at 222 nm, significantly lower than $-36\,000$ deg cm^2 $dmol^{-1}$, have been recorded for model polypeptides and naturally derived proteins [18–20].

For membrane proteins reconstituted in vesicles, this sort of analysis is frequently made exceedingly difficult due to complications arising from differential light scattering and absorption flattening. These phenomena are a consequence of the inhomogeneous refractive index of the vesicle suspension. Furthermore, as this effect is wavelength-dependent the signal attenuation is non-linear, a fact that increases the complexity of the resulting spectra [21–25]. Fasman and co-workers [24,25] have observed that transmembrane helices may exhibit larger absolute ellipticity values than those for soluble proteins, leading to maximal values of $+95\,000$ deg cm^2 $dmol^{-1}$ at 195–200 nm, $-50\,000$ deg cm^2 $dmol^{-1}$ at 208 nm and $-60\,000$ deg cm^2 $dmol^{-1}$ at 222 nm.

In order to reduce the above problems in spectral interpretation, we have obtained spectra of MscL in 1% *n*-β-octyl glucoside, 0.1% *n*-dodecyl-β-D-maltoside, and 2% sodium dodecyl sulfate micelles in 1% *n*-β-octyl glucoside. The use of several different kinds of detergents was needed to eliminate any detergent-specific influences on the CD spectra and subsequent interpretations. As seen in Fig. 2(a), the spectra in the three different detergents exhibit minima at 208 and 222 nm, indicative of a highly helical protein. The value for the ellipticity at 222 nm, $E_{222} = -45\,000$ deg cm^2 $dmol^{-1}$, is lower than that suggested for a 100% helical protein. Yet as stated

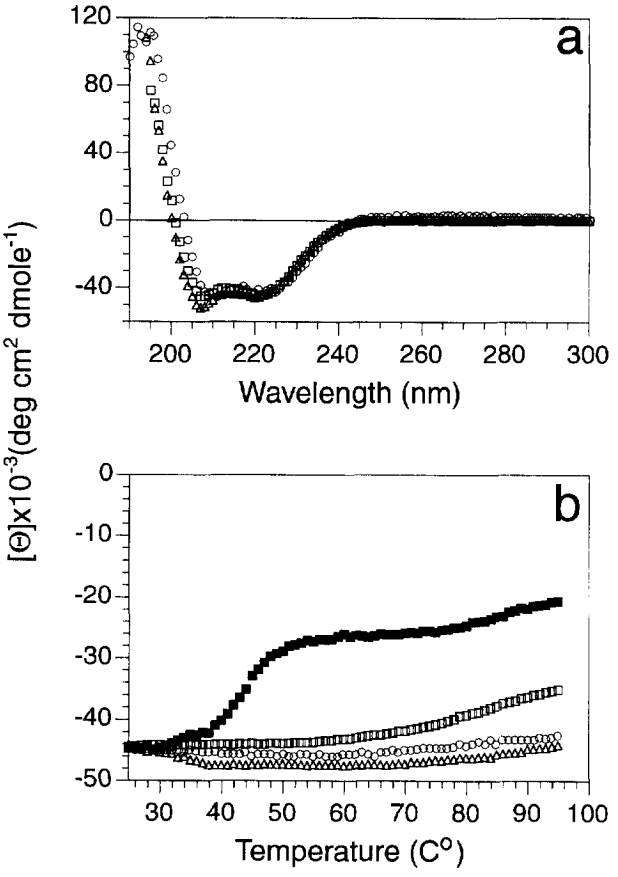

Fig. 2. (a) – Top panel shows circular dichroism spectra of MscL in three different detergent micelles: (○) 1% *n*-β-octyl glucoside, (□) 0.1% *n*-dodecyl-β-D-maltoside and (△) 1% *n*-β-octyl glucoside +2% sodium dodecyl sulfate corrected to mean residue ellipticity. 10 spectra were averaged for increased signal-to-noise ratio. (b) – Bottom panel shows the ellipticity thermal profile for MscL in (○) 1% *n*-β-octyl glucoside, (□) 0.1% *n*-dodecyl-β-D-maltoside, (△) 1% *n*-β-octyl glucoside +2% sodium dodecyl sulfate and (■) 1% *n*-β-octyl glucoside +5.3 M urea. All samples contained 1 mM $NaH_2PO_4 \cdot Na_2HPO_4$ pH 6.80 as buffer.

above, many other proteins have been shown to exhibit molar ellipticities at 222 nm significantly lower than $-36\,000\,\mathrm{deg\,cm^2\,dmol^{-1}}$ [18–20]. Thus, at present, it is only possible to state from the CD spectroscopic results that MscL is an extremely helical protein. Upper (100%) and lower (75%) bounds of the helical content can be estimated by using the maximal and minimal values for a 100% helical protein in the literature: $-36\,000$ and $-60\,000\,\mathrm{deg\,cm^2\,dmol^{-1}}$ at 222 nm, respectively [16,17,24,25].

3.1.2. Transmission Fourier transform infrared spectroscopy

Transmission Fourier transform infrared spectroscopy is another tool for analyzing the secondary structure of proteins. In contrast to CD spectroscopy, it is particularly suited for studying membrane proteins as no scattering complications persist at these long wavelengths. Here, the analysis is based on the known correlation between the frequency of the amide I vibrational mode (C=O stretch of the peptide bond) and the secondary structure. Bands centered at $1654\,\mathrm{cm^{-1}}$ correspond to α-helical structures while bands centered at $1624–1637\,\mathrm{cm^{-1}}$ and $1675\,\mathrm{cm^{-1}}$ correspond to the out-of-phase and in-phase modes of β-sheet [7] or β-turn [26] structures, respectively. (For a review on Fourier transform infrared spectroscopy spectroscopy of membrane proteins, see Ref. [27].)

The transmission Fourier transform infrared spectroscopy spectrum of MscL in dehydrated phospholipid bilayers is presented in Fig. 3 as well as the corresponding Fourier self-deconvolutions. The peak is centered at $1656\,\mathrm{cm^{-1}}$ and has a bandwidth at half height of $27.5\,\mathrm{cm^{-1}}$, both results indicating that the protein is highly helical. For example, a peak width at half height of $32 \pm 1\,\mathrm{cm^{-1}}$ is given for a 'pure' α-helical component by Venyaminov and Kalnin [8–10]. The minor peaks at 1630 and $1680\,\mathrm{cm^{-1}}$ may be attributed to β-sheet structures arising from extramembranous segments.

A more quantitative estimate of secondary structure can be derived by using the method of Venyaminov and Kalnin [8–10]. This method was recently applied to the study of three membrane proteins: EmrE [12], phospholamban [11], and diacylglycerol kinase [13] (see Section 2). It takes into account the different extinction coefficients of the different secondary structures, as well as overlapping side-chain modes. Using this methodology, we have obtained an α-helical fraction of 76–88%. The values obtained by Fourier transform infrared spectroscopy are consistent with the high helical content obtained by CD spectroscopy.

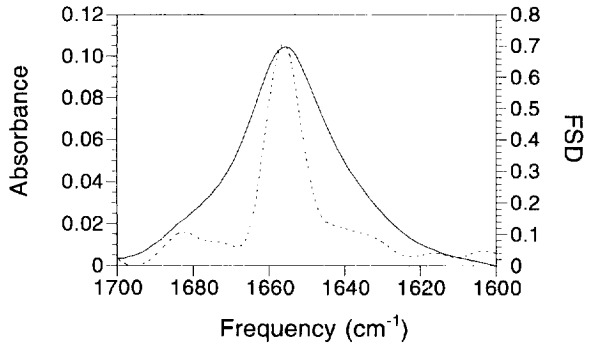

Fig. 3. Transmission FT-IR spectra of (————) MscL and (---) corresponding Fourier self-deconvolutions [6] in dehydrated DMPC vesicles in the region of the amide I vibrational mode. Fourier self-deconvolutions were obtained using an enhancement factor of 2.4 and a bandwidth of $13\,\mathrm{cm^{-1}}$ [7].

In analyzing the data, we have taken into account the fact that the protein has an affinity label consisting of six histidine residues at the carboxy terminus of the protein, that is most likely in random-coil configuration. Thus, the measured helicity is in fact lower than that in the native protein. It should be noted however, that this method employs extinction coefficients for peptides and amino acids from solution studies, while in this study the analysis was applied to dehydrated lipid films. Furthermore, additional errors may arise from the change of the extinction coefficients as a result of local structure. These factors are probably minor and are reflected in the error ranges of the extinction coefficients given by Venyaminov and Kalnin [8–10].

An additional caveat in the transition Fourier transform infrared spectroscopy measurements is that they are taken on dehydrated samples. Attenuated total-reflection Fourier transform infrared spectroscopy spectra obtained for fully hydrated MscL in lipid vesicles (see below) did not yield signal-to-noise ratios sufficient for Fourier self-deconvolution and spectral analysis as described in the foregoing (Fig. 4). However, although the spectrum of the rehydrated sample was

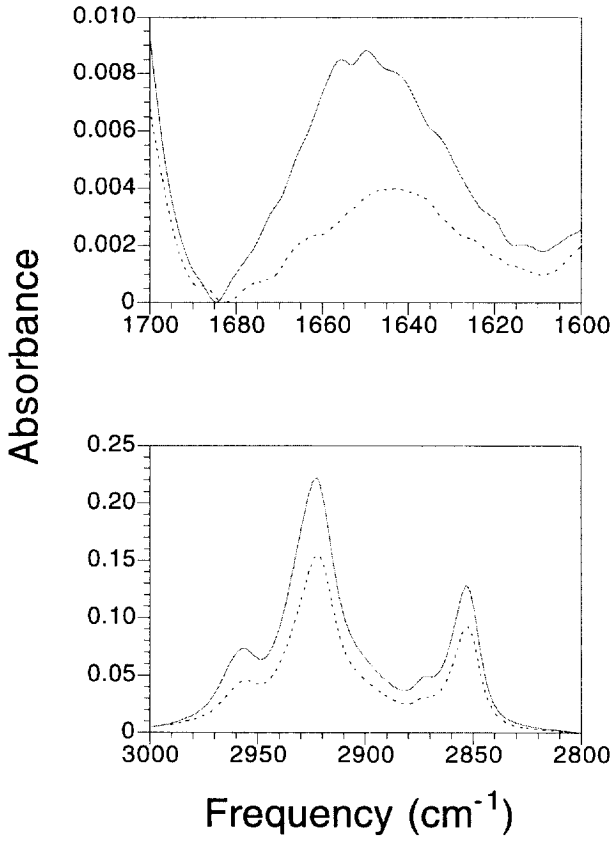

Fig. 4. Attenuated total-reflection FT-IR spectra obtained with (————) parallel or (---) perpendicular polarized light of MscL in hydrated oriented phospholipid bilayers. Top panel presents spectra in the amide I region, while the bottom panel depicts spectra in the region of the lipid methylene stretching modes.

noisy, it has the same character as that of the dehydrated one, suggesting that the secondary conformation is the same. The peak shift for the hydrated attenuated total-reflection sample of 5–10 cm^{-1} is commonly observed for proteins dissolved in D_2O [28].

3.2. Thermal stability of MscL

In order to estimate the thermal stability of the protein, an ellipticity thermal profile was collected as a function of temperature. As seen in Fig. 2(b) the magnitude of the ellipticity measured at 222 nm does not decrease with temperature both, in the nonionic (*n*-β-octyl glucoside and *n*-dodecyl-β-D-maltoside) and in the ionic (sodium dodecyl sulfate) detergents, indicating that the protein does not undergo any unfolding of its secondary structure in the region of temperatures tested (25–95°C). This high thermal stability is common for membrane proteins (e.g. Ref. [11]). This results from the fact that no other H-bonding acceptors or donors are present in the hydrophobic environment of the lipid bilayer, raising the energy 'cost' of breaking them [29]. (For a recent review on thermal stability of membrane protein, see Ref. [30].)

Adding 5.3 M urea to MscL in 1% *n*-β-octyl glucoside, resulted in a ellipticity transition taking place at ca. 43°C. Interestingly, the reduction of ellipticity and inferred helicity is just 50%, suggesting that perhaps the extra-membranous parts of the protein were unfolding while the membranous parts remain folded, as urea would denature the water-soluble parts of the protein before affecting the membrane spanning domains. The reason for the minor transition at 75°C is not clear, but may indicate a protein folding intermediate. It should also be noted that the reversibility of the transition has not been demonstrated.

As stated in the previous paragraph, although the protein remains highly helical in the disruptive ionic detergent, sodium dodecyl sulfate, it does not possess the same tertiary interactions present in the nondenaturing detergents, *n*-β-octyl glucoside and *n*-dodecyl-β-D-maltoside. Therefore, the high thermal stability of the protein is most likely a property of its monomeric structure and not of its oligomeric form.

3.3. Helical orientation

Fig. 4 presents the amide I region of the attenuated total-reflection FT-IR spectra of fully hydrated (in D_2O) MscL reconstituted in an oriented phospholipid bilayer. Spectra were obtained using parallel and perpendicular polarized light. The dichroic ratios, corresponding order parameter and calculated maximal tilt angles of the protein amide I band (Fourier self-deconvoluted spectra) as well of the lipid methylene symmetric stretching mode (2852 cm^{-1}) are listed in Table 1.

The measured order parameter for the protein amide I band ($\mathscr{S} = 0.25$) yields, upon direct calculation only, the maximal tilt angle from the bilayer

Table 1
Dichroic ratios (R^{ATR}), corresponding order parameters ($\mathscr{S}$) and calculated maximal tilt angles (θ_{max}) of the protein amide I band (Fourier self-deconvoluted spectra) as well of the lipid methylene symmetric stretching mode (2852 cm^{-1}). See Section 2 for details on data analysis

Vibrational mode	R^{ATR}	$\mathscr{S}$	θ_{max}
Protein amide I (1656 cm^{-1})	2.4	0.25, 0.65 [a]	45°, 29° [a]
Lipid CH_2 symmetric stretching mode (2852 cm^{-1})	1.4	0.4	39°

[a] Indicates order parameters and resulting maximal tilt angle corrected for bilayer disorder as indicated in the text.

normal (θ_{max}) (Table 1). This results from the fact that the bilayer order parameter is assumed to be equal to one ($\mathscr{S}_{bilayer} = 1$). The low order parameter obtained for the lipid bilayer of $\mathscr{S}_{bilayer} = 0.4$ may be used to determine the actual protein order parameter by deconvolution of the two numbers yielding a protein order parameter of $\mathscr{S} = 0.65$. Furthermore, the order parameter obtained represents all of the helical elements of the protein. Thus, it is impossible to determine whether the protein consists of one long tilted helix or a few disjointed helices, each with its unique tilt angle from the bilayer normal.

It is useful to compare the order parameter obtained for MscL to that obtained for two well-characterized 'orthogonal' membrane proteins: glycophorin A [31–36]. and melittin [37]. An order parameter of 0.35 was obtained for glycophorin A by Smith et al. [31] while an order parameter of −0.55 was reported for melittin by Frey and Tamm [28]. Glycophorin A has a net transmembrane orientation, whereas melittin adopts a conformation in which the helical director is parallel to the bilayer plane. Note, that a completely random orientation would result in an order parameter of 0. Thus, one can conclude that the order parameter obtained for MscL is consistent with a net transbilayer orientation of its helical components.

3.4. Membrane incorporation

The amount of protein embedded in the lipid bilayer can be inferred from the level of amide protons undergoing H^+/D^+ exchange, as this process takes place very slowly in the hydrophobic milieu of a lipid bilayer [27]. Detection of amide proton H^+/D^+ exchange is done by observing the reduction of the amide II vibrational mode (N–H rock at 1545 cm^{-1}), upon concentration normalization using the intensity of the amide I band as a standard.

Spectra resulting from this experiment are shown in Fig. 5. The reduction in the amide II band (roughly 66%) and the shift in the peak of the amide I vibrational mode by −4 cm^{-1} indicate that, out of 142 amino acids of the protein, only ca. 48 are protected from H^+/D^+ exchange. Similar results were obtained for MscL in 5.3 M urea (data not shown). This result is in contrast to that observed for highly embedded membrane proteins such as bacteriorhodopsin, whereby only 40% of the amide proton undergo H^+/D^+ exchange [38]. This fraction of exchanging residues in bacteriorhodopsin correlated well with membranous residues identified in the three-dimensional structure of bacteriorhodopsin [39]. These results suggest that two-thirds of MscL are water accessible. A contribution to amide H^+/D^+ exchange may arise from residues located in the ion pore. Even though the H^+/D^+ exchange was under-

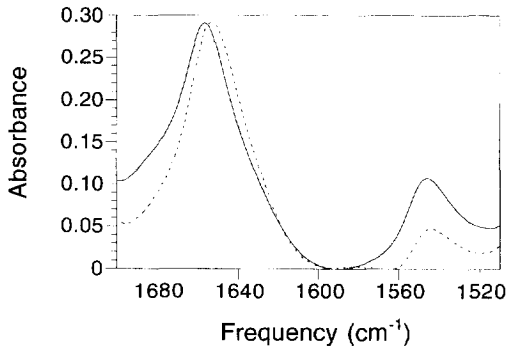

Fig. 5. Transmission FT-IR spectra of MscL in DMPC vesicles dried from either (————) H_2O or (- - -) in D_2O in the region of the amide I and amide II vibrational modes. Spectra are normalized according to the size of the amide I mode as an indicator of protein concentration. Amide proton H^+/D^+ exchange is visualized by a reduction of the amide II vibrational mode corresponding to the peptide bond N–H rocking motion.

taken in conditions that would render the channel in the closed state of the channel, a large vestibule may persist enabling solvent penetration into the ion pore.

3.5. Structural implications

The spectroscopic data can be summarized as follows:

1. MscL is a highly helical protein with roughly 111 amino acids in α-helical configuration (82 ± 6% using the secondary structure estimate from the Fourier transform infrared spectroscopy and from CD).
2. No reduction in secondary structure content is seen in the temperature range tested (25–95°C), as commonly observed for membrane proteins.
3. The helical elements of MscL are oriented in a net transbilayer orientation.
4. Only one-third of the protein is protected from amide H^+/D^+ exchange by the lipid bilayer.

These data along with the analysis of the protein sequence [2] and topology [3] are consistent with a helix–loop–helix model of MscL subunit structure. The two putative transmembrane segments (M1 : L19-A38 and M2 : A70 : I96) are roughly similar in size to the number of amino acids protected from H^+/D^+ exchange. The rest of the protein, also helical, is found to be water-exposed, or at least water-accessible. Does this result contradict the observed high stability of the protein secondary structure to denaturing agents (25–95°C, 2% SDS) which is typical mainly for membrane-embedded hydrophobic proteins such as bacteriorhodopsin? It is known that membrane-spanning helical segments of MscL may remain stable because the helix-keeping hydrogen bonds are stronger in a nonpolar environment [29]. One can speculate that the conformation of the periplasmic loop, yet unknown, may be important for maintaining the fold of the solvent-exposed regions under these conditions.

The simplest model of MscL consists of a bundle of two anti-parallel helices. Since the helicity of the protein is not reduced even at 95°C, one can assume that the helical elements are continuous and nucleated by the highly stable transmembrane segments. This behavior has been observed with the protein phospholamban, in which the transmembrane helices confer thermal stability to the cytoplasmic helices [11]. However, the periplasmic part of MscL contains helix-breaking (Pro-Pro) and hinge-like (Gly-Gly) sequences, so the loop may bend to the membrane surface or, alternatively, dip into the channel interior similar to the hypothesized P-segments of most voltage-gated channels [40]. In the latter case, the net transmembrane orientation of helices would also be satisfied, but more than two structural elements would be interacting. The loop contacting the two hydrophobic helices may form a more stable structure than the free loop. Taking into account the exceptionally large conductance of the channel, it may have a wide aqueous vestibule providing access for H^+/D^+ exchange. Further studies of the periplasmic loop conformation by a number of independent techniques may bring new insights to structure-functional relationships of this new class of channels.

Acknowledgements

This work was funded in part by a grant to Axel T. Brünger from NIH (GM-54160-01) and a grant to Sergei Sukharev from NASA (NAGW-4934).

References

[1] S. Sukharev, B. Martinac, V. Arshavsky, C. Kung, Biophys J. 65 (1) (1993) 177–183.
[2] S. Sukharev, P. Blount, B. Martinac, F. Blattner, C. Kung, Nature 368 (6468) (1994) 265–268.
[3] P. Blount, S. Sukharev, P. Moe, M. Schroeder, H. Guy, C. Kung, BMBO J. 15 (1996) 4798–4805.
[4] M. Innis, D. Gelfand, J. Sninsky, T. White, PCR Protocols. A Guide to Methods and Applications, 1st edn., Academic Press, Inc., San Diego, 1990.
[5] K. Chumakov, M. Rozanov, V. Agol, Eur. J. Biochem. 127 (2) (1982) 309–314.
[6] J. Kauppinen, D. Moffatt, H. Mantsch, D. Cameron, Appl. Spectrosc. 35 (1982) 271–276.
[7] D. Byler, H. Susi, Biopolymers 25 (3) (1986) 469–487.
[8] N. Kalnin, I. Baikalov, S. Venyaminov, Biopolymers 30 (13–14) (1990) 1273–1280.
[9] S. Venyaminov, N. Kalnin, Biopolymers 30 (13–14) (1990) 1243–1257.
[10] S. Venyaminov, N. Kalnin, Biopolymers 30 (13–14) (1990) 1259–1271.
[11] I. Arkin, M. Rothman, C. Ludlam, S. Aimoto, D. Engelman, K. Rothschild, S. Smith, J. Mol. Biol. 248 (4) (1995) 824–834.

[12] I. Arkin, W. Russ, M. Lebendiker, S. Schuldiner, Biochem. 35 (1996) 7233–7238.
[13] C. Sanders, L. Czerski, O. Vinogradova, P. Badola, D. Song, S. Smith, Biochem. 25 (26) (1996) 8610–8618.
[14] N. Harrick, Interbal Reflection Spectroscopy, 1st edn., Interscience Publishers, New York, 1967.
[15] M. Tsuboi, J. Polymer Sci. 59 (1962) 139–153.
[16] I. Tinoco, R. Woody, D. Bradley, J. Chem. Phys. 38 (1963) 1137–1325.
[17] Y. Chen, J. Yang, K. Chau, Biochem. 13 (16) (1974) 3350–3359.
[18] J. Cassim, J. Yang, Biopolymers 9 (12) (1970) 1475–1502.
[19] L. Kostrikis, D. Liu, L. Day, Biochem. 33 (7) (1994) 1694–1703.
[20] E. Gazit, A. Boman, H. Boman, Y. Shai, Biochem. 34 (36) (1995) 11479–11488.
[21] L. Duysens, Biochim. Biophys. Acta 19 (1956) 1–12.
[22] M. Long, D. Urry, Membrane Spectroscopy, 1st edn. Springer-Verlag, Berlin.
[23] D. Mao, B. Wallace, Biochem. 23 (12) (1984) 2667–2673.
[24] K. Park, A. Perczel, G. Fasman, Protein Sci. 1 (8) (1992) 1032–1049.
[25] G. Fasman, Biotechnol. Appl. Biochem. 18 (Pt 2) (1993) 111–138.
[26] S. Krimm, J. Bandekar, Biopolymers 19 (1) (1980) 1–29.
[27] M. Braiman, K. Rothschild, Annu. Rev. Biophys. Biophys. Chem. 17 (1988) 541–570.
[28] S. Frey, L. Tamm, Biophys. J. 60 (4) (1991) 922–930.
[29] D. Engelman, T. Steitz, A. Goldman, Annu. Rev. Biophys. Biophy. Chem. 15 (1986) 321–353.
[30] T. Haltia, E. Freire, Biochim. Biophys. Acta 1228 (1) (1995) 1–27.
[31] S. Smith, R. Jonas, M. Braiman, B. Bormann, Biochem. 33 (20) (1994) 6334–6341.
[32] S. Smith, B. Bormann, Proc. Natl. Acad. Sci. USA 92 (2) (1995) 488–491.
[33] M. Lemmon, J. Flanagan, H. Treutlein, J. Zhang, D. Engelman, Biochem. 31 (51) (1992) 12719–12725.
[34] M. Lemmon, J. Flanagan, J. Hunt, B. Adair, B. Bormann, C. Dempsey, D. Engelman, J. Biol. Chem. 267 (11) (1992) 7683–7689.
[35] M. Lemmon, H. Treutlein, P. Adams, A. T. Brünger, D. Engelman, Nat. Struct. Biol. 1 (3) (1994) 157–163.
[36] H. Treutlein, M. Lemmon, D. Engelman, A. T. Brünger, Biochem. 31 (51) (1992) 12726–12732.
[37] C. Dempsey, Biochim. Biophys. Acta 1031 (2) (1990) 143–161.
[38] J. Torres, F. Sepulcre, E. Padros, Biochem. 34 (1995) 16320–16326.
[39] R. Henderson, J. Baldwin, T. Ceska, F. Zemlin, E. Beckmann, K. Downing, J. Mol. Biol. 213 (4) (1990) 899–929.
[40] L. Jan, Y. Jan, Nature 371 (6493) (1994) 119–122.